

Heparin-like Polysaccharides Reduce Osteolytic Bone Destruction and Tumor Growth in a Mouse Model of Breast Cancer Bone Metastasis

Sirkku Pollari¹, Rami S. Käkönen³, Khalid S. Mohammad⁵, Jukka P. Rissanen³, Jussi M. Halleen³, Anni Wärrä², Liisa Nissinen⁴, Marjo Pihlavisto⁴, Anne Marjamäki⁴, Merja Perälä¹, Theresa A. Guise⁵, Olli Kallioniemi^{1,6}, and Sanna-Maria Käkönen²

Abstract

TGF- β regulates several steps in cancer metastasis, including the establishment of bone metastatic lesions. TGF- β is released from bone during osteoclastic bone resorption and it stimulates breast cancer cells to produce osteolytic factors such as interleukin 11 (IL-11). We conducted a cell-based siRNA screen and identified heparan sulfate 6-O-sulfotransferase 2 (HS6ST2) as a critical gene for TGF- β -induced IL-11 production in highly bone metastatic MDA-MB-231(SA) breast cancer cells. HS6ST2 attaches sulfate groups to glucosamine residues in heparan sulfate glycosaminoglycans. We subsequently showed how heparin and a high-molecular-weight *Escherichia coli* K5-derived heparin-like polysaccharide (K5-NSOS) inhibited TGF- β -induced IL-11 production in MDA-MB-231(SA) cells. In addition, K5-NSOS inhibited bone resorption activity of human osteoclasts *in vitro*. We evaluated the therapeutic potential of K5-NSOS and fragmin in a mouse model of breast cancer bone metastasis. MDA-MB-231(SA) cells were inoculated into the left cardiac ventricle of athymic nude mice which were treated with fragmin, K5-NSOS, or vehicle once a day for four weeks. Both heparin-like glycosaminoglycans inhibited weight reduction, decreased osteolytic lesion area, and reduced tumor burden in bone. In conclusion, our data imply novel mechanisms involved in TGF- β induction and support the critical role of heparan sulfate glycosaminoglycans in cancer metastasis as well as indicate that K5-NSOS is a potential antimetastatic and antiresorptive agent for cancer therapy. This study illustrates the potential to translate *in vitro* siRNA screening results toward *in vivo* therapeutic concepts. *Mol Cancer Res*; 10(5); 597–604. ©2012 AACR.

Introduction

Most patients with breast cancer in advanced stages of the disease have bone metastases with painful symptoms caused by fractures and nerve compression syndromes. The majority of bone metastases are osteolytic, resulting from cancer-induced increased osteoclast activity in bone (1). Cancer cell invasion and metastasis to distant sites is highly dependent on the ability of metastatic cells to respond to local paracrine growth factors in the different microenvironments they encounter, as well as on their ability to produce and respond

to autocrine growth factors. TGF- β is a key regulator of several steps in the metastatic cascade such as epithelial-to-mesenchymal transition and tumor cell invasion. In the bone microenvironment, TGF- β is released from bone during osteoclastic bone resorption and it stimulates tumor cell growth and production of osteolytic factors such as interleukin (IL)-11, PTHrP, and VEGF. Previous studies have showed that blockade of TGF- β signaling by small molecule inhibitors against the type I TGF- β receptor kinase activity or neutralizing antibodies against TGF- β is an effective way to prevent and treat bone metastases in preclinical models (2). However, total systemic blockade of this pathway may cause off-target effects as TGF- β has many functions in normal physiology and may also act as a tumor suppressor in certain malignancies, including early stages of breast cancer.

To prevent the undesired effects caused by enhanced TGF- β signaling in breast cancer, we aimed to identify critical mediators of the pathway and conducted an siRNA screen in highly bone metastatic MDA-MB-231(SA) cells. We used a library of siRNAs targeting the genes that we had found to be most highly overexpressed in MDA-MB-231(SA) versus parental MDA-MB-231 cells. One of the siRNAs that inhibited TGF- β -induced IL-11 production

Authors' Affiliations: ¹Medical Biotechnology, VTT Technical Research Centre of Finland and Turku Centre for Biotechnology, ²Institute of Biomedicine, University of Turku; ³Pharmatest Services Ltd; ⁴Biotie Therapies Corp., Turku, Finland; ⁵Indiana University, Indianapolis, Indiana; and ⁶Institute for Molecular Medicine Finland (FIMM), University of Helsinki, Helsinki, Finland

Note: Supplementary data for this article are available at Molecular Cancer Research Online (<http://mcr.aacrjournals.org/>).

Corresponding Author: Sirkku Pollari, VTT Technical Research Centre of Finland and Turku Centre for Biotechnology, University of Turku, PO Box 106, Turku 20520, Finland. Phone: 358-2-4788-605; Fax: 358-20-722-2840; E-mail: sielpo@utu.fi

doi: 10.1158/1541-7786.MCR-11-0482

©2012 American Association for Cancer Research.

targeted heparan sulfate 6-*O*-sulfotransferase 2 (HS6ST2), an enzyme that attaches sulfate groups to glucosamine residues in heparan sulfate. Therefore, we subsequently evaluated the effects of exogenous highly sulfated heparan sulfate glycosaminoglycans on TGF- β induction of IL-11. Highly sulfated heparan sulfate glycosaminoglycans, such as heparin, are commonly used to prevent venous thromboembolism, which is a common complication in patients with cancer as well. Heparin and heparin-like glycosaminoglycans (HLGAGs) have also been shown to prolong survival of patients with cancer, suggesting an antimetastatic effect for these compounds (3–5). The applicability of heparin in cancer therapy is limited because of its strong anticoagulant activity, but HLGAGs with less undesired effects on blood coagulation have been developed. Two HLGAGs with low anticoagulant activity, a low-molecular-weight (LMW) heparin fragmin and a high-molecular-weight (HMW) *E. coli* K5-derived heparin-like polysaccharide (K5-NSOS) were used in our studies. In addition to analyzing the effects of these HLGAGs on TGF- β -induced IL-11 production, we studied their *in vivo* antimetastatic properties in a mouse model of breast cancer bone metastasis and effects on osteoclast activity *in vitro*.

Materials and Methods

Cell culture

MDA-MB-231(SA) cells were comprehensively characterized by comparative genomic hybridization and genome-wide gene expression profiling by our research group as described in (6). The cells were cultured in Dulbecco's Modified Eagle's Medium supplemented with 10% inactivated calf serum, 1% penicillin/streptomycin, and nonessential amino acids at +37°C in a humidified incubator in an atmosphere of 5% CO₂.

siRNA transfection and IL-11 and cell viability assays

Cells were transfected with siRNAs (Qiagen) at a final concentration of 15 (384-well plates) or 20 nmol/L (96-well plates). Briefly, the siRNAs were robotically printed to black 384-well clear-bottom plates or manually pipetted to black 96-well clear-bottom plates. siLentFect transfection agent (Bio-Rad Laboratories) diluted in OptiMEM (Gibco Invitrogen) was added into each well. After a 60-minute incubation at room temperature, 1,400 (384-well plates) or 10,000 (96-well plates) cells per well were added. After 24 hours, medium was changed and heparin, fragmin, or K5-NSOS (0.25 mg/mL) and TGF- β (5 ng/mL) were added. IL-11 concentration in the conditioned medium and cell viability were measured 24 hours later using the DuoSet ELISA Development System for human IL-11 (R&D Systems) and CellTiter-Blue assay (Promega), respectively, according to the manufacturers' instructions.

Quantitative reverse transcription RT-PCR

RNA isolation, reverse transcription, and TaqMan analyses were done as previously described (6). The primers and probes are listed in the Supplementary Table S1.

Smad luciferase reporter assays

Smad signaling was quantified using the Cignal Smad Reporter Assay Kit (SABiosciences). siRNAs (10 nmol/L) along with 93-ng luciferase reporter construct were cotransfected into MDA-MB-231(SA) cells using 0.47 μ L Lipofectamine 2000 (Invitrogen). Medium was replaced with serum-free medium 18 hours after transfection, and 5 ng/mL TGF- β was added 23 to 27 hours later. Activity of the firefly luciferase reporter and *Renilla* luciferase was measured after 6- to 10-hour TGF- β induction using the Dual-Glo Luciferase Assay System (Promega Corporation) according to the manufacturer's instructions. The background signal from the untransfected cells was subtracted, and the firefly reporter values were divided with the respective *Renilla* values.

Heparin and HLGAGs

Heparin from porcine intestinal mucosa was obtained from LEO Pharma and LMW heparin dalteparin (fragmin) from Pharmacia (ATC code B01A04, molecular weight 4–6 kDa). The HMW chemically *N, O*-sulfated bacterial polysaccharide (capsular polysaccharide from *E. coli* K5) was prepared as described in (7). The overall sulfation degree (sulfate groups per disaccharide unit) of the prepared K5-NSOS derivative was more than 3.5 and the molecular weight approximately 37 kDa.

Mouse bone metastasis model

Effects of fragmin and K5-NSOS on the development of bone metastases were studied using a previously described mouse model of osteolytic breast cancer bone metastasis (8, 9). Female nude mice (BALB/c *nul/nul*; Harlan) 4 to 5 weeks of age were inoculated with 100,000 MDA-MB-231(SA) cells into the left cardiac ventricle. Mice were administered with fragmin s.c. and K5-NSOS i.v. (5 mg/kg diluted in sterile water) or sterile water as a control ($n = 11, 7, \text{ and } 10$ mice per group, respectively) at the time of cell inoculation and daily thereafter. The mice were maintained in a pathogen-free environment and monitored daily for clinical signs. Animal studies were conducted in accordance with the institutional animal care protocol or University of Texas Health Science Center at San Antonio (San Antonio, TX). Body weight was obtained at baseline and then weekly for 4 weeks, at which time the mice were sacrificed. Necropsy was conducted on all mice, and those with tumor in the chest were excluded from analysis because this indicated that the tumor inoculum did not properly enter the left cardiac ventricle. At sacrifice, hind and fore limbs and soft tissues were collected for histologic analysis.

Radiographic analyses

Development of bone metastases was monitored weekly by X-ray radiography. The animals were anaesthetized with Ketamine-Xylazine cocktail and X-rayed in a prone position with the Faxitron Specimen Radiographic System MX-20 DC-2 (Faxitron Corporation). The total lesion number and area in hind (left and right tibia and femur) and fore (left and right humerus) limbs per mouse were quantified from the images using MetaMorph image analysis software.

(Molecular Devices Corporation). All radiographs were evaluated without knowledge of treatment groups.

Histology and histomorphometry

The tissue samples were fixed in 10% neutral-buffered formalin for 2 to 3 days. The soft tissue samples were then stored at 70% ethanol, and the bone samples were decalcified in 14% EDTA for 2 weeks. After embedding in paraffin, 3.5 μ m tissue sections were cut using a standard microtome. Tissue sections were placed on poly-L-lysine-coated glass slides and stained with hematoxylin and eosin (H&E) using standard histologic staining procedures. Some sections were stained with tartrate-resistant acid phosphatase (TRAP)-stained for determining the number of osteoclasts. Total tumor areas were measured from midsagittal sections of tibiae, femora, and humerus. Total tumor area and total bone area per bone were determined using MetaMorph image analysis software. In addition, the number of osteoclasts per millimeter of tumor–bone interface in midsections of tibiae and femora was determined. Histomorphometry was conducted without knowledge of treatment groups.

Osteoclast cultures

Human osteoclast precursors (Poietics, Cambrex) were cultured on bovine bone slices (Nordic Bioscience Diagnostics) in 96-well plates for 10 days according to the manufacturer's instructions. After the osteoclasts' differentiation period, at day 7, the culture medium was replaced with fresh medium and different concentrations of fragmin or K5-NSOS were added. Osteoclasts were cultured for an additional 3 days. To determine the number of osteoclasts, TRACP 5b activity was measured from the medium collected at day 7 using the BoneTRAP Assay (IDS Ltd). At day 10, the amount of CTX (C-terminal telopeptide of α 1 collagen) released from bone was quantified from the medium using CrossLaps for Culture assay (Nordic Bioscience Diagnostics). Resorption index was calculated by dividing the CTX values (day 10) by the TRACP 5b values (day 7; ref. 10). Multinuclear TRACP-positive osteoclasts were visualized by staining the nuclei with Hoechst 33258 (Sigma-Aldrich) and TRACP content of the cells using a leukocyte acid phosphatase kit (Sigma-Aldrich). Resorption pits were visualized using TRITC-conjugated WGA lectin (L-5266, Sigma), as previously explained (11). A cysteine protease inhibitor E64 (Sigma) was used as a reference inhibitor of osteoclast activity, as previously described (12).

In vitro coagulation tests

Anti-IIa and anti-Xa activities of fragmin, heparin, and K5-NSOS were determined using Chromogenic IL Test Heparin assay kit according to the manufacturer's protocol and ACL 7000 automated coagulation analyzer (both from Instrumentation Laboratory Company). In the assays, the residual factors IIa and Xa were quantified with a synthetic chromogenic substrate. The buffer solution 0.9% NaCl was used in the anti-Xa activity measurements whereas buffer solution 0.05 mol/L Tris, 0.15 mol/L NaCl, 1% (w/v) bovine serum albumin, PH 7.4 was used in the anti-IIa

measurements. The compounds were measured against an international LMW heparin standard ("Low-Molecular-Mass Heparin", European Pharmacopoeia Commission). The effects of fragmin, heparin, and K5-NSOS on activated partial thromboplastin time (APTT) in citrated plasma were measured using IL Test APTT Lyophilized silica kit (ILS Laboratories Scandinavia Oy) according to the manufacturer's instructions. Dose–response curves as clotting time versus test compound concentration were prepared, and the doses causing a coagulation time of 100 seconds (APTT_{100s}) were estimated from the trend lines.

Statistical analysis

The *in vitro* data are shown as mean \pm SD and *in vivo* data as mean \pm SEM. Data were analyzed for statistical significance by one-way ANOVA followed by the Student *t* test or the Dunnett test or by nonparametric Kruskal–Wallis test followed by the Dunn comparison. *P* values less than 0.05 were considered statistically significant.

Results

Identification of genes whose expression is critical to TGF- β -induced IL-11 production in MDA-MB-231 (SA) cells

We noted an increased basal and TGF- β -induced IL-11 secretion in the highly bone metastatic MDA-MB-231(SA) variant as compared with the parental MDA-MB-231 breast cancer cell line (Supplementary Fig. S1). We used the genome-wide gene expression profiles of these cell types (6) and constructed a library consisting of 193 siRNAs targeting 107 genes (1 validated or 2 nonvalidated siRNAs per gene) that were most highly overexpressed in MDA-MB-231(SA) versus parental cells. In addition, we included a scrambled sequence siRNA as a negative control and 2 IL-11 siRNAs as positive controls. The most potent inhibitors of TGF- β -induced IL-11 secretion were confirmed using multiple replicates (Supplementary Table S2 and Fig. S2A). One such hit was an siRNA-targeting HS6ST2 (Fig. 1A and B). This gene encodes an enzyme that attaches sulfate groups to C-6 of glucosamine residues in heparan sulfate glycosaminoglycans. We confirmed the overexpression of HS6ST2 in the highly metastatic MDA-MB-231(SA) versus parental cells by quantitative RT-PCR (Supplementary Fig. S3A). We also studied whether other enzymes that attach sulfate groups to glucosamine residues in heparan sulfate glycosaminoglycans affect IL-11 secretion. Our data showed that knockdown of HS6ST1 had a similar effect as HS6ST2 silencing whereas knockdown of HS3ST1 slightly increased IL-11 secretion (Supplementary Fig. S2B). The knockdown efficiencies of the siRNAs were measured by quantitative RT-PCR (Supplementary Fig. S3B).

HS6ST2 silencing inhibits Smad signaling

Because TGF- β induction of IL-11 has been shown to be mediated by the Smad pathway (13, 14), we tested whether silencing of HS6ST2 affected Smad2/3/4-mediated transcriptional activity. This was done using a luciferase reporter

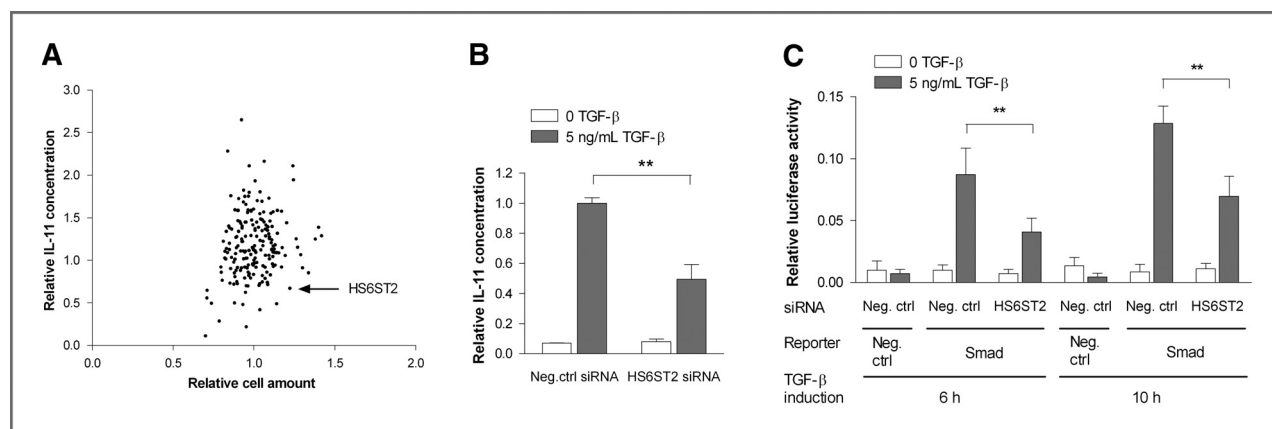


Figure 1. Identification of siRNAs that inhibit TGF- β -induced IL-11 production in MDA-MB-231(SA) cells. A, the effects of 196 siRNAs on TGF- β -induced IL-11 production and cell viability [cell amount relative to negative control (neg. ctrl) siRNA]. B, the effect of HS6ST2 knockdown (siRNA product ID SI00442232) on IL-11 production ($n = 3$). C, the effect of HS6ST2 knockdown on Smad signaling ($n = 4$). **, $P < 0.01$ (t test).

construct containing a functional Smad-binding site. HS6ST2 silencing suppressed the TGF- β -induced luciferase signal, indicating a decrease in Smad binding to its response element (Fig. 1C).

Heparin and a HLGAG K5-NSOS inhibit TGF- β -induced IL-11 production in MDA-MB-231(SA) cells

It has been shown that TGF- β 1 binds to heparin and highly sulfated liver heparan sulfate, and this potentiates the biologic activity of TGF- β 1 (15–17). It is also well established that heparan sulfate–protein interactions critically depend on the amount and the positions of the sulfate groups (18). We therefore hypothesized that exogenous highly sulfated heparan sulfates, such as heparin and HLGAGs, may interfere with the physiologic heparan sulfate–TGF- β interactions and affect TGF- β signaling. Our *in vitro* data showed that heparin and a HMW HLGAG K5-NSOS inhibited TGF- β -induced IL-11 production in MDA-MB-231(SA) cells ($P < 0.001$) whereas a LMW HLGAG fragmin did not show a significant effect (Fig. 2).

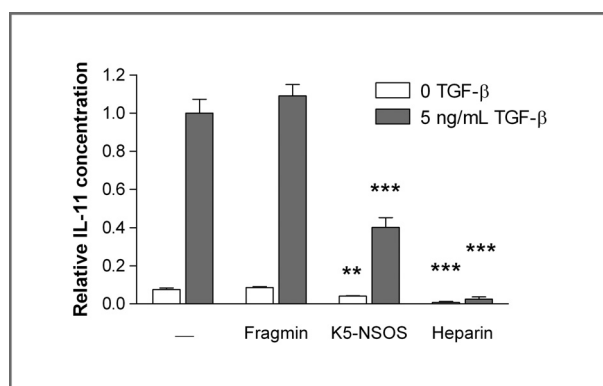


Figure 2. The effects of fragmin, K5-NSOS, and heparin on IL-11 production in MDA-MB-231(SA) cells ($n = 3$). **, $P < 0.01$; ***, $P < 0.001$ (t test), as compared with the respective control without compound treatment.

K5-NSOS and fragmin inhibit weight reduction and reduce cachexia in tumor-bearing animals

We evaluated the therapeutic potential of K5-NSOS and fragmin in a mouse model of breast cancer bone metastasis. The mice that had been inoculated with MDA-MB-231(SA) cells were treated with fragmin, K5-NSOS, or vehicle at the time of MDA-MB-231(SA) cell inoculation and daily thereafter. The vehicle group had markedly lower body weight at sacrifice than in the baseline body weight due to tumor-induced cachexia. In contrast, the body weights of the fragmin- and K5-NSOS-treated mice at sacrifice were significantly higher than the vehicle group ($P < 0.01$ and $P < 0.001$; Fig. 3A). Furthermore, only 18% of the fragmin-treated mice and 29% of the K5-NSOS-treated mice were cachectic as compared with 86% of the vehicle-treated mice at sacrifice.

K5-NSOS and fragmin reduce osteolytic lesions and tumor growth in bone

Osteolytic lesion area as measured by radiographs was significantly lower in the fragmin- and K5-NSOS-treated groups than the vehicle group at sacrifice ($P < 0.001$; Fig. 3B and C). Histomorphometric examination revealed a significant reduction in tumor burden in bone in both heparin-like compound-treated groups as compared with the vehicle group (Fig. 3D and E). The total tumor area as determined per mouse was significantly smaller in both treatment groups than in the vehicle group ($P < 0.05$; Fig. 3E). Treatment with the heparin-like compounds did not have any significant effect on the size of the bone area or osteoclast number per mm tumor–bone interface as compared with the vehicle group (data not shown).

K5-NSOS and fragmin have different effects on human osteoclast activity *in vitro*

We also studied the effects of HLGAGs on human osteoclasts. Osteoclast precursors were cultured on bovine bone slices, and after the 7-day differentiation period, fragmin or K5-NSOS was added to the culture medium.

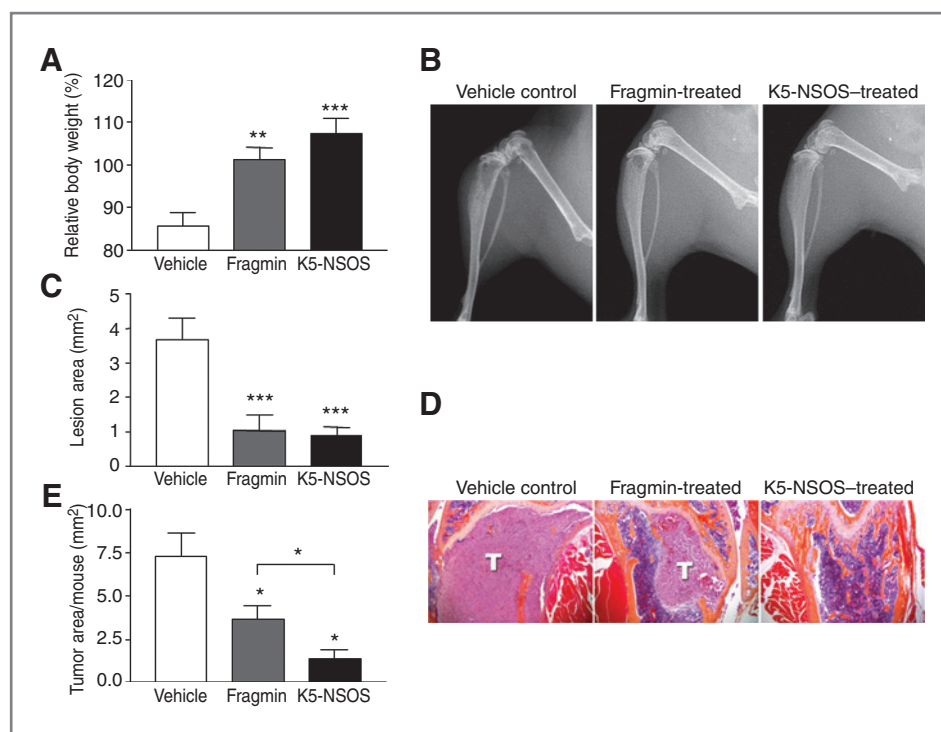


Figure 3. Heparin-like compounds inhibit weight reduction as well as reduce tumor-induced osteolysis and tumor growth in bone in a mouse model of breast cancer bone metastasis. A, body weight at sacrifice compared with the baseline body weight of the control ($n = 10$), fragmin- ($n = 11$), and K5-NSOS-treated ($n = 7$) mice. B, representative X-ray images of the control, fragmin-, and K5-NSOS-treated groups at sacrifice. C, osteolytic lesion area was determined by radiography in hind and fore limbs in the control ($n = 10$), fragmin- ($n = 11$), and K5-NSOS-treated ($n = 7$) groups. D, representative figures ($\times 4$ magnification) of H&E-stained proximal tibiae of control, fragmin-treated, and K5-NSOS-treated groups at sacrifice. T, tumor. E, tumor area as determined by histomorphometry in H&E-stained sections of tibia and femora of the control- ($n = 10$), fragmin- ($n = 11$), and K5-NSOS-treated ($n = 7$) mice. *, $P < 0.05$; **, $P < 0.01$; ***, $P < 0.001$ (ANOVA followed by the Dunnett test).

Fragmin did not affect osteoclast activity as determined by the resorption index CTX/TRACP 5b, whereas a dose-dependent inhibitory effect was observed with K5-NSOS (Fig. 4).

K5-NSOS has lower anticoagulant activity than fragmin

The applicability of heparin in cancer therapy is limited because of its anticoagulant activity. We compared the anticoagulant properties of K5-NSOS, fragmin, and heparin by measuring the antithrombin (anti-IIa) and antifactor Xa activity (anti-Xa), which are specific coagulation parameters typically determined for heparin-like molecules. Fragmin and heparin showed the expected anti-IIa and anti-Xa activity. Only moderate anti-IIa and anti-Xa activity was observed with K5-NSOS. In addition, the effects of fragmin and K5-NSOS on APTT were tested as a function of concentration. K5-NSOS had clearly weaker prolonging effect on APTT than heparin. The concentration of K5-NSOS required to prolong APTT_{100s} was almost equal to that of fragmin (Table 1).

Discussion

Our previous comparative genomic hybridization and genome-wide gene expression analyses indicated that the

MDA-MB-231(SA) variant is closely related to the parental MDA-MB-231 cell line despite its remarkably enhanced bone metastatic propensity *in vivo* (6). Because TGF- β and IL-11 are important regulators of the metastatic process in the bone microenvironment and there is an increased TGF- β -induced IL-11 production in the MDA-MB-231(SA) as compared with the parental cells, we aimed to identify critical mediators of this induction among the genes that were highly overexpressed in the MDA-MB-231(SA) variant. One of the most highly overexpressed genes whose knockdown inhibited TGF- β -induced IL-11 production was HS6ST2. We subsequently showed that silencing of HS6ST2 inhibited Smad2/3/4-mediated transcriptional activity. The Smad pathway has previously been shown to be essential for IL-11 induction by TGF- β (13). HS6ST2 encodes an enzyme that attaches sulfate groups to glucosamine residues in heparan sulfate. Heparan sulfate glycosaminoglycans consist of a repeat disaccharide unit of either iduronic or glucuronic acid linked to a glucosamine. Distinct sulfation and acetylation patterns of *O*- and *N*-positions within the disaccharide units determine binding sites for numerous growth factors and cytokines (19, 20). Also TGF- β 1 has been shown to bind to highly sulfated heparan sulfate glycosaminoglycans *in vitro*. Binding potentiates the biologic activity of TGF- β by protecting TGF- β 1 from proteolytic degradation (17) and

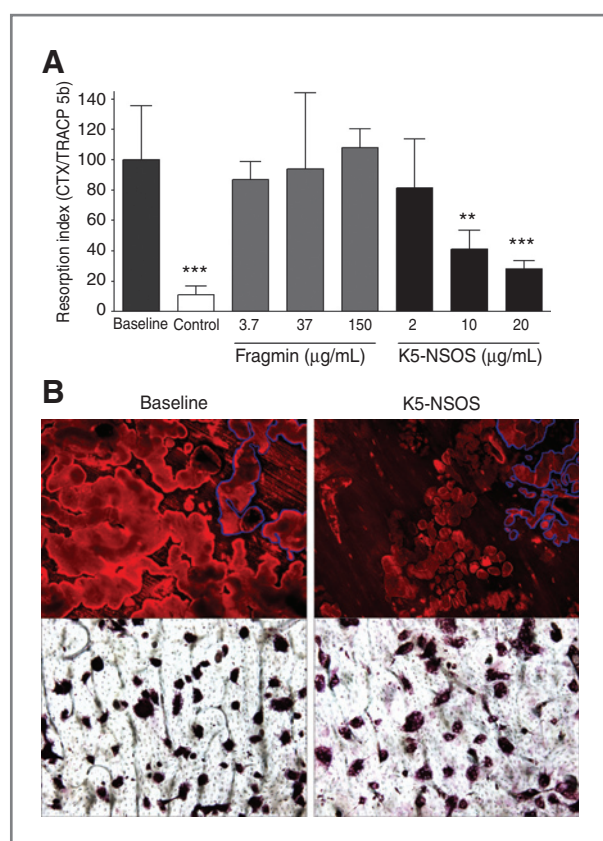


Figure 4. Heparin-like compounds have different effects on osteoclast activity *in vitro*. A, the effects of fragmin and K5-NSOS on the resorption index CTX (day 10)/TRACP 5b (day 7). Black bar, baseline without any compounds; white bar, a cysteine protease inhibitor E64 (positive control); light gray bars, fragmin; dark gray bars, K5-NSOS ($n = 6$ in all data points). **, $P < 0.01$; ***, $P < 0.001$ (ANOVA followed by t test), as compared with the baseline. B, representative figures of baseline and K5-NSOS-treated bone slices. The top images show WGA-stained resorption pits ($\times 20$ magnification) and the bottom images show TRACP-positive osteoclasts ($\times 10$ magnification). Examples of resorption pits are outlined in blue in the top figures.

by preventing the formation of inactive complexes with $\alpha 2$ -macroglobulin (15, 16). We found that silencing of enzymes that attach sulfate groups to C-6 of glucosamine residues, HS6ST1 and HS6ST2, inhibited TGF- β induc-

tion of IL-11. Interestingly, an enzyme responsible for the sulfation of the C-3 of glucosamine residues, HS3ST1, slightly increased TGF- β -induced expression of IL-11. We hypothesized that exogenous highly sulfated heparan sulfate glycosaminoglycans, such as heparin, could interfere with the interactions between TGF- β and cell surface heparan sulfate glycosaminoglycans and thereby inhibit TGF- β signaling. Indeed, our data showed that heparin and a chemically sulfated bacterial polysaccharide K5-NSOS with more than 90% sulfation degree at C-6 inhibited TGF- β -induced IL-11 production in MDA-MB-231(SA) cells. Fragmin did not show a similar effect which might be due to its lower molecular weight and consequently reduced interaction capacity.

Intracardiac injection of MDA-MB-231 human breast cancer cells into nude mice is a well-established model for breast cancer bone metastasis. We used this model and observed a significant inhibition of tumor growth in bone in the mice treated with K5-NSOS or fragmin. The antimetastatic effects of these compounds were also observed as a reduction in tumor-induced cachexia and as an increase in body weight in the mice treated with HLGAGs. Tumor-induced bone destruction was significantly reduced by both HLGAGs. These data extend previous observations that have implicated antimetastatic effects for heparin and HLGAGs in animal model systems (21–26). Clinical studies have also indicated that heparin and HLGAGs may prolong survival of patients with cancer with solid tumors (3–5).

The complex coupling mechanisms between bone resorption and formation during the normal and tumor cell-induced bone remodeling make studies on the effects of HLGAGs on bone challenging. Furthermore, the mice used in this study were still growing and consequently had increased bone remodeling *per se*. Both fragmin and K5-NSOS reduced tumor-induced osteolysis as shown by the decreased lesion area in the X-ray radiographs. However, we did not see overall effect on total bone area. This could be due to the fact that the total bone area (both cortical and trabecular) was measured across the whole bone and not at the metaphysis resulting in dilution of the bone preservation effect of the drug that is noticeable particularly at the metaphysis. We also did not see a statistical

Table 1. Coagulation activities of fragmin and K5-NSOS *in vitro*

Compound	Anti-Xa, IU/mg	Anti-IIa, IU/mg	APTT _{100s} , μ g/mL
K5-NSOS	14	6	10.9
Fragmin	155	74	9.4
Heparin	148	132	0.5

NOTE: The coagulation tests were conducted using the IL Test Heparin or the APTT Lyophilized Silica Kit. Anti-Xa and anti-IIa activities were determined by monitoring the level of paranitroaniline released from the chromogenic substrate in the enzyme reaction at 405 nm. APTT_{100s} was determined by preparing dose-response curves as clotting time versus test compound concentration. The concentration required to prolong the coagulation time to 100s was estimated from the dose-response curve. All measurements were made according to the International Low-Molecular-Mass Heparin standard.

difference in osteoclast number per bone surface between the vehicle and treatment group. This parameter was assessed at the tumor–bone interface, and because in the vehicle control group there was more bone destruction at the metaphysis, this probably resulted in reduction in the osteoclast number similar to that seen by the compound treatment.

Previous studies have indicated that heparin and HLGAGs might have adverse effects on bone. Osteoporosis is a well-recognized complication of high-dose or long-term heparin therapy (27–29). Heparin has been shown to promote bone resorption by increasing the activity and number of osteoclasts and to inhibit bone formation by decreasing osteoblast function and number of osteoblasts both *in vitro* and *in vivo* (30–34). LMW heparin-like compounds appear to cause less adverse effects on bone than in unfractionated heparin (reviewed in ref. 35). Size and sulfation of the heterogeneous group of HLGAGs are suggested to be the major determinants of their ability to promote bone resorption (34) and suppress bone formation (30). The 2 HLGAGs used in our study differed both in their size and sulfation degree. The LMW heparin, fragmin, has a molecular weight of approximately 5 kDa and the highly sulfated K5-NSOS approximately 37 kDa. Fragmin has been shown to stimulate osteoclast activity and inhibit osteoblast activity less than unfractionated heparin (30, 34, 36). In line with the previous findings, our results showed that fragmin did not significantly affect osteoclast activity in human osteoclast cultures. Surprisingly, a dose-dependent inhibition of osteoclast resorption activity was observed with K5-NSOS even though a lower dose compared with fragmin was used. As shown by our results, the reduced resorption was not due to toxic effect on osteoclasts. This unexpected antiresorptive effect of K5-NSOS warrants further studies in nontumor-bearing animals.

Heparin and LMW HLGAGs have been used as anticoagulants for decades, and their clinical risk benefit profiles are well understood and acceptable but the ability to exploit heparin and HLGAGs in cancer therapy has been limited by their anticoagulant activity. We showed that K5-NSOS had lower anticoagulant activity than fragmin, as indicated by 11 times lower anti-Xa and 12 times lower anti-IIa activity. In addition, K5-NSOS had a weak prolonging effect on APTT, indicating a weak influence on global

plasma coagulation. These properties of K5-NSOS make it substantially more applicable than heparin and other anticoagulants as a cancer therapeutic agent.

Taken together, our data imply novel mechanisms involved in TGF- β induction in breast cancer cells and support the critical role of heparan sulfate glycosaminoglycans in cancer metastasis. Highly sulfated heparin-like compounds K5-NSOS and fragmin efficiently reduce osteolytic lesion area and metastatic tumor burden in bone as well as have beneficial effects on body weight and tumor-related cachexia in a mouse model of breast cancer bone metastasis. K5-NSOS only and not fragmin reduces TGF- β -induced IL-11 production in cancer cells and inhibits bone resorption activity of osteoclasts which might explain the significantly more efficient inhibition of osteolysis and tumor burden by K5-NSOS than by fragmin. In conclusion, K5-NSOS is a potential antimetastatic and antiresorptive agent with low anticoagulant activity. Additional modification of the size and sulfation degree of K5-NSOS could further lower its anticoagulant activity (7, 37) and improve its applicability as a therapeutic agent to prevent and treat breast cancer metastases.

Disclosure of Potential Conflicts of Interest

R.S. Kähkönen has ownership interest (including patents) for Pharmatest Services shares. No potential conflicts of interest were disclosed by the other authors.

Acknowledgments

The authors thank late Markku Salmivirta, MD, PhD for fruitful scientific discussions related to the K5-NSOS development and Michele Carreon, Barry Grubbs, Maryla Niewolna, Beryl Story, Yong Cui (University of Texas Health Science Center at San Antonio, San Antonio, TX), Marika Ojala (Biotie Therapies Corp.), and Suvi Suutari (Pharmatest Services Ltd.) for excellent technical assistance.

Grant Support

This work was supported by Academy of Finland, Verein zur Förderung der Krebsforschung (TIME project), Finnish Cancer Organisations, and Sigrid Jusélius Foundation (to O. Kallioniemi); Drug Discovery Graduate School, Finnish Cultural Foundation, and Cancer Society of Southwestern Finland (to S. Pollari); NIH grants R01CA69158, R01DK067333, R01DK065837, and U01CA143057, the Mary Kay Ash Foundation, the V-Foundation, the Jerry W. and Peggy S. Throgmartin Endowment of Indiana University, the Indiana Economic Development Fund, and Susan Komen Foundation (to T.A. Guise).

The costs of publication of this article were defrayed in part by the payment of page charges. This article must therefore be hereby marked *advertisement* in accordance with 18 U.S.C. Section 1734 solely to indicate this fact.

Received October 3, 2011; revised February 21, 2012; accepted March 6, 2012; published OnlineFirst April 20, 2012.

References

- Kozlow W, Guise TA. Breast cancer metastasis to bone: Mechanisms of osteolysis and implications for therapy. *J Mammary Gland Biol Neoplasia* 2005;10:169–80.
- Mohammad KS, Javelaud D, Fournier PG, Niewolna M, McKenna CR, Peng XH, et al. TGF- β -RI kinase inhibitor SD-208 reduces the development and progression of melanoma bone metastases. *Cancer Res* 2011;71:175–84.
- Hettiarachchi RJ, Smorenburg SM, Ginsberg J, Levine M, Prins MH, Buller HR. Do heparins do more than just treat thrombosis? the influence of heparins on cancer spread. *Thromb Haemost* 1999;82:947–52.
- Kakkar AK, Levine MN, Kadziola Z, Lemoine NR, Low V, Patel HK, et al. Low molecular weight heparin, therapy with dalteparin, and survival in advanced cancer: The fragmin advanced malignancy outcome study (FAMOUS). *J Clin Oncol* 2004;22:1944–8.
- Klerk CP, Smorenburg SM, Otten HM, Lensing AW, Prins MH, Piovella F, et al. The effect of low molecular weight heparin on survival in patients with advanced malignancy. *J Clin Oncol* 2005;23:2130–5.

6. Pollari S, Kakonen SM, Edgren H, Wolf M, Kohonen P, Sara H, et al. Enhanced serine production by bone metastatic breast cancer cells stimulates osteoclastogenesis. *Breast Cancer Res Treat* 2011;125:421–30.
7. Casu B, Grazioli G, Razi N, Guerrini M, Naggi A, Torri G, et al. Heparin-like compounds prepared by chemical modification of capsular polysaccharide from *E. coli* K5. *Carbohydr Res* 1994;263:271–84.
8. Arguello F, Baggs RB, Frantz CN. A murine model of experimental metastasis to bone and bone marrow. *Cancer Res* 1988;48:6876–81.
9. Guise TA, Yin JJ, Taylor SD, Kumagai Y, Dallas M, Boyce BF, et al. Evidence for a causal role of parathyroid hormone-related protein in the pathogenesis of human breast cancer-mediated osteolysis. *J Clin Invest* 1996;98:1544–9.
10. Rissanen JP, Ylipahkala H, Fagerlund KM, Long C, Vaananen HK, Halleen JM. Improved methods for testing antiresorptive compounds in human osteoclast cultures. *J Bone Miner Metab* 2009;27:105–9.
11. Selander K, Lehenkari P, Vaananen HK. The effects of bisphosphonates on the resorption cycle of isolated osteoclasts. *Calcif Tissue Int* 1994;55:368–75.
12. Delaisse JM, Eeckhout Y, Vaes G. Inhibition of bone resorption in culture by inhibitors of thiol proteinases. *Biochem J* 1980;192:365–8.
13. Kang Y, He W, Tulley S, Gupta GP, Serganova I, Chen CR, et al. Breast cancer bone metastasis mediated by the smad tumor suppressor pathway. *Proc Natl Acad Sci U S A* 2005;102:13909–14.
14. Gupta J, Robbins J, Jilling T, Seth P. TGFbeta-dependent induction of interleukin-11 and interleukin-8 involves SMAD and p38 MAPK pathways in breast tumor models with varied bone metastases potential. *Cancer Biol Ther* 2011;11:311–6.
15. Lyon M, Rushton G, Gallagher JT. The interaction of the transforming growth factor-betas with heparin/heparan sulfate is isoform-specific. *J Biol Chem* 1997;272:18000–6.
16. McCaffrey TA, Falcone DJ, Brayton CF, Agarwal LA, Welt FG, Weksler BB. Transforming growth factor-beta activity is potentiated by heparin via dissociation of the transforming growth factor-beta/alpha 2-macroglobulin inactive complex. *J Cell Biol* 1989;109:441–8.
17. McCaffrey TA, Falcone DJ, Vicente D, Du B, Consigli S, Borth W. Protection of transforming growth factor-beta 1 activity by heparin and fucoidan. *J Cell Physiol* 1994;159:51–9.
18. Nakato H, Kimata K. Heparan sulfate fine structure and specificity of proteoglycan functions. *Biochim Biophys Acta* 2002;1573:312–8.
19. Fernig DG, Gallagher JT. Fibroblast growth factors and their receptors: An information network controlling tissue growth, morphogenesis and repair. *Prog Growth Factor Res* 1994;5:353–77.
20. Lyon M, Gallagher JT. Hepatocyte growth factor/scatter factor: a heparan sulphate-binding pleiotropic growth factor. *Biochem Soc Trans* 1994;22:365–70.
21. Borgenstrom M, Warri A, Hillesvuo K, Kakonen R, Kakonen S, Nissinen L, et al. O-sulfated bacterial polysaccharides with low anticoagulant activity inhibit metastasis. *Semin Thromb Hemost* 2007;33:547–56.
22. Borsig L, Wong R, Feramisco J, Nadeau DR, Varki NM, Varki A. Heparin and cancer revisited: Mechanistic connections involving platelets, P-selectin, carcinoma mucins, and tumor metastasis. *Proc Natl Acad Sci U S A* 2001;98:3352–7.
23. Kragh M, Binderup L, Vig Hjarnaa PJ, Bramm E, Johansen KB, Frimundt Petersen C. Non-anti-coagulant heparin inhibits metastasis but not primary tumor growth. *Oncol Rep* 2005;14:99–104.
24. Poggi A, Rossi C, Casella N, Bruno C, Sturiale L, Dossi C, et al. Inhibition of B16-BL6 melanoma lung colonies by semisynthetic sulfaminoheparosan sulfates from *E. coli* K5 polysaccharide. *Semin Thromb Hemost* 2002;28:383–92.
25. Szende B, Paku S, Racz G, Kopper L. Effect of fraxiparine and heparin on experimental tumor metastasis in mice. *Anticancer Res* 2005;25:2869–72.
26. Yee CK, Butcher M, Zeadin M, Weitz JI, Shaughnessy SG. Inhibition of osteolytic bone metastasis by unfractionated heparin. *Clin Exp Metastasis* 2008;25:903–11.
27. Douketis JD, Ginsberg JS, Burrows RF, Duku EK, Webber CE, Brill-Edwards P. The effects of long-term heparin therapy during pregnancy on bone density. A prospective matched cohort study. *Thromb Haemost* 1996;75:254–7.
28. Hawkins D, Evans J. Minimising the risk of heparin-induced osteoporosis during pregnancy. *Expert Opin Drug Saf* 2005;4:583–90.
29. Nelson-Piercy C. Heparin-induced osteoporosis. *Scand J Rheumatol Suppl* 1998;107:68–71.
30. Bhandari M, Hirsh J, Weitz JI, Young E, Venner TJ, Shaughnessy SG. The effects of standard and low molecular weight heparin on bone nodule formation *in vitro*. *Thromb Haemost* 1998;80:413–7.
31. Kock HJ, Handschin AE. Osteoblast growth inhibition by unfractionated heparin and by low molecular weight heparins: An *in-vitro* investigation. *Clin Appl Thromb Hemost* 2002;8:251–5.
32. Muir JM, Andrew M, Hirsh J, Weitz JI, Young E, Deschamps P, et al. Histomorphometric analysis of the effects of standard heparin on trabecular bone *in vivo*. *Blood* 1996;88:1314–20.
33. Nishiyama M, Itoh F, Ujiie A. Low-molecular-weight heparin (dalteparin) demonstrated a weaker effect on rat bone metabolism compared with heparin. *Jpn J Pharmacol* 1997;74:59–68.
34. Shaughnessy SG, Young E, Deschamps P, Hirsh J. The effects of low molecular weight and standard heparin on calcium loss from fetal rat calvaria. *Blood* 1995;86:1368–73.
35. Rajgopal R, Bear M, Butcher MK, Shaughnessy SG. The effects of heparin and low molecular weight heparins on bone. *Thromb Res* 2008;122:293–8.
36. Handschin AE, Trentz OA, Hoerstrup SP, Kock HJ, Wanner GA, Trentz O. Effect of low molecular weight heparin (dalteparin) and fondaparinux (arixtra) on human osteoblasts *in vitro*. *Br J Surg* 2005;92:177–83.
37. Rusnati M, Oreste P, Zoppetti G, Presta M. Biotechnological engineering of heparin/heparan sulphate: a novel area of multi-target drug discovery. *Curr Pharm Des* 2005;11:2489–99.

Molecular Cancer Research

Heparin-like Polysaccharides Reduce Osteolytic Bone Destruction and Tumor Growth in a Mouse Model of Breast Cancer Bone Metastasis

Sirkku Pollari, Rami S. Kähkönen, Khalid S. Mohammad, et al.

Mol Cancer Res 2012;10:597-604. Published OnlineFirst April 20, 2012.

Updated version Access the most recent version of this article at:
doi:[10.1158/1541-7786.MCR-11-0482](https://doi.org/10.1158/1541-7786.MCR-11-0482)

Supplementary Material Access the most recent supplemental material at:
<http://mcr.aacrjournals.org/content/suppl/2012/03/15/1541-7786.MCR-11-0482.DC1>

Cited articles This article cites 37 articles, 12 of which you can access for free at:
<http://mcr.aacrjournals.org/content/10/5/597.full#ref-list-1>

Citing articles This article has been cited by 1 HighWire-hosted articles. Access the articles at:
<http://mcr.aacrjournals.org/content/10/5/597.full#related-urls>

E-mail alerts [Sign up to receive free email-alerts](#) related to this article or journal.

Reprints and Subscriptions To order reprints of this article or to subscribe to the journal, contact the AACR Publications Department at pubs@aacr.org.

Permissions To request permission to re-use all or part of this article, use this link
<http://mcr.aacrjournals.org/content/10/5/597>.
Click on "Request Permissions" which will take you to the Copyright Clearance Center's (CCC) Rightslink site.